Comparison of Shared Class I HLA-Bound Noncanonical Neoepitopes between Normal and Neoplastic Tissues of Pancreatic Adenocarcinoma

Tengyi Zhang[1,2,3,4], Betul Celiker[1,2,3,4], Yingkuan Shao[1,2,5], Jessica Gai[1,2,3,4], Mark Hill[6], Chunyu Wang[7,8], and Lei Zheng[1,2,3,4,9,10]

ABSTRACT

Purpose: Developing T-cell or vaccine therapies for pancreatic ductal adenocarcinoma (PDAC) has been challenging because of a lack of knowledge regarding immunodominant, cancer-specific antigens as PDAC are characterized by a scarcity of genomic mutation-associated neoepitopes, and effective approaches to discover them are limited.

Experimental Design: An advanced mass spectrometry approach was employed to compare the immunopeptidome of PDAC tissues and matched normal tissues from the same patients.

Results: This study identified HLA class I–binding variant peptides derived from canonical proteins, which had single amino-acid substitutions not attributed to genetic mutations or RNA editing. These amino-acid substitutions appeared to result from translational errors. The variant peptides were predominantly found in tumor tissues, with certain peptides common among multiple patients. Importantly, several of these variant peptides were more immunogenic than their wild-type counterparts.

Conclusions: The shared noncanonical neoepitopes identified in this study offer promising candidates for vaccine and T-cell therapy development, potentially providing new avenues for immunotherapy in PDAC.

See related commentary by Yuan et al., p. 1821

Introduction

Pancreatic ductal adenocarcinoma (PDAC) is the third leading cause of cancer-related death in the United States with a dismal 5-year survival rate of 12% (1, 2). With only 15% to 20% of patients with PDAC eligible for surgery at diagnosis, the quest for novel and effective therapies for patients with PDAC stands as a paramount concern. Immunotherapy has recently emerged as a promising avenue in cancer treatment; however, its effectiveness on PDAC is hindered by the lack of effector T cells in the tumor microenvironment (TME; ref. 3). One of the strategies for overcoming the PDAC resistance to immunotherapy involves identifying immunogenic tumor-associated antigens (TAA) and tumor-specific antigens (TSA) for the development of personalized cancer vaccines and T cell–based therapies (4).

Numerous clinical trials have investigated the efficacy of targeting TAAs through cancer vaccines and T cell-based therapies (5, 6). Examples of PDAC TAAs currently under clinical investigations of therapeutic targets include epitopes derived from MUC1, Mesothelin, and Annexin A2 (7). However, TAAs are non-mutated self-antigens that are also expressed in normal healthy tissues, and therapies targeting these antigens can result in either immune tolerance or "off-tumor toxicity" events that destroy normal tissues, causing serious and even fatal side effects(8). In contrast, TSAs or neoantigens are exclusively expressed in cancer tissue, arising from genetic, epigenetic, or other noncanonical mutations (9). Compared with TAAs, neoantigens present better therapeutic prospects owing to their tumor-specific expression, absence in normal tissues, and heightened immunogenicity stemming from their lack of expression in medullary thymic epithelial cells (mTEC), where central tolerance is established (9–11). A recent study by Rojas and colleagues (12) demonstrated that adjuvant autogene cevumeran, an individualized neoantigen vaccine, was able to induce safe and sustained neoantigen-specific T-cell response in 50% of the unselected patients with resectable PDAC when administered with atezolizumab and mFOLFIRNOX. However, given their individualistic origins from tumor mutations, neoantigen-based immunotherapy usually necessitates personalized production of vaccine for each patient and thus the delay of adjuvant chemotherapy (13).

Currently, the prediction of neoepitopes depends on genomic analysis, such as the whole exome sequencing (WES) data (14).

[1]Sidney Kimmel Comprehensive Cancer Center, Johns Hopkins University School of Medicine, Baltimore, Maryland. [2]Department of Oncology, Johns Hopkins University School of Medicine, Baltimore, Maryland. [3]Pancreatic Cancer Precision Medicine Center of Excellence Program, Johns Hopkins University School of Medicine, Baltimore, Maryland. [4]Bloomberg-Kimmel Institute for Cancer Immunotherapy, Johns Hopkins University School of Medicine, Baltimore, Maryland. [5]Department of Breast Surgery and Oncology, Key Laboratory of Cancer Prevention and Intervention, Cancer Institute, Ministry of Education, Second Affiliated Hospital, Zhejiang University School of Medicine, Hangzhou, China. [6]Immuno-Oncology Discovery and Translational Medicine, Bristol Myers Squibb Company, Seattle, Washington. [7]Department of Biological Sciences, Center for Biotechnology and Interdisciplinary Studies, Rensselaer Polytechnic Institute, Troy, New York. [8]Department of Chemistry and Chemical Biology, Center for Biotechnology and Interdisciplinary Studies, Rensselaer Polytechnic Institute, Troy, New York. [9]Department of Surgery, Johns Hopkins University School of Medicine, Baltimore, Maryland. [10]The Cancer Convergence Institute at Johns Hopkins, Johns Hopkins University School of Medicine, Baltimore, Maryland.

Corresponding Author: Lei Zheng, Johns Hopkins University School of Medicine, 7979 Wurzbach Road, MC8026, San Antonio, TX 78229. E-mail: Lzheng6@jhmi.edu

Clin Cancer Res 2025;31:1956–65

doi: 10.1158/1078-0432.CCR-24-2251

Translational Relevance

Using advanced mass spectrometry methods, this study identified PDAC-specific neoantigens characterized by enhanced immunogenicity, thereby offering promising prospects for targeted immunotherapy. These noncanonical neoepitopes, absent in normal tissues, underscore the potential for personalized treatment strategies. Despite challenges associated with off-tumor effects in targeting tumor-associated antigens, our focus on tumor-specific antigens or neoantigens presents a viable solution. Our findings pave the way for the development of safer and more effective neoantigen-based treatments in pancreatic cancer, aiming to mitigate off-tumor effects. This approach not only enhances specificity but also addresses current PDAC immunotherapy limitations, potentially leading to improved clinical outcomes and enhanced survival rates.

Although this approach allows the identification of neoepitopes that arise from genomic variations, it would not detect neoepitopes resulting from nongenomic variants such as post-translational modification, defective ribosomal products (DRiP), proteasome splicing, and other nongenomic alterations (14–19). To the best of our knowledge, whether noncanonical neoepitopes could arise from alterations in the translational process has never been studied. Translation errors leading to single-amino acid substitutes can be caused by erroneous charging of a transfer RNA (tRNA) with a "noncognate" amino acid by its partner tRNA synthetase or failed ribosomal recognition of codon–anticodon pairing in its A-site (20). Such errors occur when a specific amino acid is underrepresented, or one specific type of tRNA is overabundant. Recent work by Pataskar and colleagues (21) shed light on one such mechanism by showing that enriched tryptophan-to-phenylalanine (W > F) substitutes were driven by tryptophan-depletion-induced alternative tRNA aminoacylation in various cancers, including PDAC. Interestingly, this study demonstrated that epitopes with this amino acid substitution exhibited heightened surface antigen presentation and could induce potent T-cell recognition and activation, underlining the potential for discovering neoepitopes arising from erroneous translation.

In our previous work, using advanced mass spectrometry (MS) analysis, we successfully identified natural HLA class I– and class II–binding epitopes in the neoplastic tissues of PDAC (22). Our prior research further validated the *in vitro* and *in vivo* antitumor activity of T cells expressing the T-cell receptor (TCR) specific for one of the HLA class I epitope, $LAMC2_{203–211}$, confirming the feasibility of using MS to identify $CD8^+$ T-cell epitopes for the development of TCR T-cell therapies. In this present study, we employed the same MS analytical methods to compare the immunopeptidome of PDAC tissues and their corresponding normal tissue from the same patients. We further identified tumor-restricted epitopes with no normal tissue expression. Furthermore, to identify neoepitopes not present in the current proteomics databases, we adapted Novor, a *de novo* peptide sequencing algorithm that derives peptide sequences directly from the MS/MS spectrum without referencing a sequence database (23). Through this approach, we identified HLA class I–binding variant peptides derived from canonical proteins with single amino-acid substitutes, which were shared by multiple patients and may become noncanonical shared neoantigens.

Materials and Methods

Cell culture

Authenticated W6/32 cells (RRID:CVCL_7872) and T2 cells (RRID:CVCL_2211) were purchased from American Type Culture Collection (ATCC) and maintained by following the protocols suggested by ATCC. Mycoplasma testing was performed every 6 months. T2-A3 and T2-A11 cells were genetically modified from T2 cells, a human B and T lymphoblast hybrid expressing only the HLA-A2 allele, to express the HLA-A3 and HLA-A11 alleles, respectively.

Human tissues and specimens

Human PDAC resection and normal pancreatic specimens were obtained from the patients who underwent surgery at the Johns Hopkins Hospital under the Johns Hopkins Medical Institution (JHMI) Institutional Review Board (IRB) approved protocol (IRB00244430), and through the Rapid Autopsy Program (RAP) Shared Resource (SR) at The Sidney Kimmel Comprehensive Cancer Center. This program was approved by the Johns Hopkins IRB and deemed in compliance with the Health Insurance Portability and Accountability Act. Written informed consent from patients involved in the work was obtained in accordance with U.S. Common Rule.

Preparation of antibody conjugated affinity purification columns

The antibody conjugated affinity purification columns were prepared following a modified protocol described in detail previously (24, 25). W6/32 cells were cultured to produce pan-HLA-I (A, B, C; ref. 26). The cell culture supernatant containing the antibodies were diluted with Pierce Protein A (for anti-HLA class I affinity column) or protein G (for anti-HLA class II affinity column) binding buffer (Thermo Scientific). The diluted supernatant was then passed through columns packed with Pierce Protein A Plus Agarose beads (Thermo Scientific). The columns were first washed with the respective binding buffers and then with 0.2 mol/L sodium borate buffer (pH 9), before the agarose beads were cross-linked with dimethyl pimelimidate (DMP; Thermo Scientific) at the final concentration of 20 mmol/L in sodium borate buffer. Unreacted DMP was quenched by rotating the beads for 2 hours in 2.5× beads volume of 200 mmol/L ethanolamine (pH8). The beads were then washed with binding buffer and stored in phosphate-buffered saline at 4°C.

Purification of HLA-bound peptides

The tissues weighing between 100 and 1,000 mg were flash frozen in liquid nitrogen after surgical resection and stored at −80°C. The tissue was ground using a mortar and a pestle and incubated in 1 to 2 mL Pierce IP lysis buffer (Thermo Scientific) containing a Complete Protease Inhibitor Cocktail (Roche) at 4°C with constant agitation for 2 hours The supernatant from the lysate was collected after 30 minutes centrifugation at 16,000 *g*, followed by an incubation with unconjugated protein A beads at 4°C for 1 hour to block nonspecific binding. The collected supernatant was then incubated with pan-HLA-I antibody conjugated protein A beads (1/10th lysate volume) overnight at 4°C while rotating slowly.

After the incubation, the beads were then washed with Buffer A containing 150 mmol/L NaCl, 20 mmol/L Tris–HCl at a 10X beads volume, Buffer B containing 400 mmol/L NaCl, 20 mmol/L Tris–HCl at a 10X beads volume, Buffer A again at a 10X beads volume,

and finally 20 mmol/L Tris–HCl (pH 8) at a 7X beads volume twice at 4°C. The HLA-peptide complexes were eluted at room temperature with 500 μL of 0.1 N acetic acid (pH 3) for 15 minutes, twice. The eluent (1 mL) containing the HLA-peptide complexes were then loaded to a Sep-Pak C18 3 cc/200 mg Vac Cartridge (Waters) that was pre-activated with 1 mL of methanol and washed with 1 mL 0.1% Trifluoroacetic acid (TFA) three times. After passing through the cartridge, the flow-through were repeatedly loaded to the cartridges two more times. To obtain the purified peptide separated from the HLA molecule, the cartridges were washed twice with 300 μL of 0.1% TFA. After washing, the peptides were then eluted for three times with 400, 300, and 30 μL L of 80% Acetonitrile in 0.1% TFA, respectively, into a clean 1.5 mL Eppendorf tube. The eluted samples were dried thoroughly at 30°C using vacuum centrifugation and then stored at −80°C. Samples were prepared in a blinded randomized manner to ensure unbiased handling and analysis during the study.

LC–MS/MS analysis of HLA peptides

LC–MS/MS analysis of eluted peptides was performed by the Mass Spectrometry and Proteomics Core at the Johns Hopkins University School of Medicine, and it was previously described by Zhang and colleagues (27). Briefly, dried eluted HLA peptides were rehydrated and loaded into an EasyLC autosampler coupled with an Orbitrap Lumos mass spectrometer (Thermo Fisher, RRID:SCR_020562). 10 μL of the sample was injected onto a trap column subsequently eluted into the mass spectrometer. The mass spectrometer operated at resolutions of 120,000 (MS) and 30,000 (MS2). Peptides were fragmented with 30% collision energy using a 1.6 Dalton isolation window. Peptides with charges 2 to 6 underwent 3-second cycle fragmentation before the next MS precursor scan. Previously fragmented precursors were excluded dynamically for 15 seconds. The MS AGC target was 4e5 ions with a maximum injection time of 50 ms; MS2 was set to 1e5 ions and 100 ms maximum. Precursor mass calibration was performed using the Easy-IC fluoranthene lock mass system.

MS data analysis of HLA peptides

MaxQuant software (https://www.maxquant.org/, RRID:SCR_014485) was used to search the mass spectrum peak lists against the UniProt databases (Human 93,609 entries, February 2018, RRID:SCR_002380) following previously described settings (26, 28). Novor, a real-time peptide *de novo* sequencing software (https://novor.cloud/, RRID:SCR_014507) was used to sequence new peptides from the tandem MS data (23). Enzyme specificity was set as unspecific. A false discovery rate of 0.01 was minimally required. The initially allowed mass deviation of the precursor ion was set to 6 p.p.m. The maximum fragment mass deviation was set to 20 p.p.m. Carbamidomethyl (C) was set as a fixed post-translational modification (PTM), and Oxidation (W3), Phospho (ST), Acetyl (N-term), Phospho (Y) were set as variable PTM. Fragmentation was set to HCD. Results obtained from Novor were searched against Swiss-Prot database in MS-Homology (University of California, San Francisco, San Francisco, Ca, RRID:SCR_014558) to identify peptides with single amino acid substitutions. Enzyme specificity was set as unspecific.

Sequence-based HLA-A typing

Extracted genomic DNA from patient tissues were amplified using a GeneQuery HLA-A PCR+Sanger SBT Typing Kit (ScienCell). The kit creates three amplicons of the *HLA-A* gene: Exon 2, Exon 3, and Exon 4. Subsequent Sanger Sequencing was performed with an Applied Biosystems 3730xl DNA Analyzer (Thermo Scientific) by the Genetic Resources Core Facility at the Johns Hopkins University of Medicine (RRID:SCR_010581). The acquired sequences are aligned to an HLA allele database using the SOAP-Typing software (BGI Genomics, RRID:SCR_024848) to obtain the four-digit genotypes of the samples.

T2 peptide binding assay

T2 cells expressing the HLA molecule of interest were resuspended in an equal mix of serum-free AimV (Fisher Scientific) and culture media [Gibco RPMI 1640 (Invitrogen) with 10% heat inactivated FCS (Geminibio), 1% L-glutamine (Geminibio) and 1% penicillin/streptomycin (Geminibio)] to a concentration of 1×10^6 cells/mL and pulsed with β-2 microglobulin (final concentration at 1.5 μg/mL, Sigma-Aldrich) and peptide (final concentration at 50 μg/mL) at room temperature with gentle shaking overnight. Cell surface MHC molecules stabilized by the peptide binding were quantified by a CytoFLEX flow cytometer (Beckman Coulter, Brea, CA, RRID:SCR_019627) with anti-HLA-A11 or A3 mouse monoclonal antibodies (One Lambda) as primary antibodies, respectively, and a rabbit anti-mouse FITC-conjugated IgG secondary antibody (Dako, RRID:AB_2532147). Dead cells were stained with the Live Dead Aqua Dead Cell Kit (Invitrogen) and excluded during analysis. Flow cytometry results were analyzed using the CytExpert software (Beckman Coulter, RRID:SCR_017217) and were presented as an increase in mean fluorescence intensity (MFI) of cells that were cultured with peptides.

FloroSpot assay

The peptides were stocked in 100% DMSO and diluted in the cell culture medium to yield a final peptide concentration at 10 ng/mL. Archived, cryopreserved PBMCs were recovered and immediately subjected to the FloroSpot assay. The FloroSpot assays were performed using the Human IFNg/ TNFa/IL-2 FSP-0110 kits (Mabtech) by the Immune Monitoring Core at the Johns Hopkins University School of Medicine. Plates were read by an AID iSpot Spectrum reader (Autoimmun Diagnostika GmbH, RRID:SCR_025287), and the results were processed by the software provided by the manufacturer.

Three-dimensional structural prediction

Alphafold (https://alphafold.ebi.ac.uk/, RRID:SCR_025454; refs. 29, 30) was used to predict the peptide-MHC structures, which were then visualized using ChimeraX 1.6.1 (RRID:SCR_015872). HLA molecule sequence was obtained from IPD-IMGT/HLA (https://www.ebi.ac.uk/ipd/imgt/hla/, RRID:SCR_002971): HLA-A*03:01 (HLA00038) and HLA-A*33:01 (HLA00105). Wild-type and variant peptide sequences were identified using MS-Homology (https://msviewer.ucsf.edu/mshome.htm, RRID:SCR_014558) following LC–MS/MS analysis of eluted peptides from patient samples.

Statistical analyses

All statistical analyses and graphs were made using GraphPad Prism 9.5.1 software (GraphPad Software, RRID:SCR_002798). Unpaired *t* test was used for comparing the MFI of different peptides in the T2 peptide binding assay. For the florospot assay, the mean values of spot forming units (SFU) were compared using Welch's *t* test for two-group comparisons and by one-way analysis of variance for multiple group comparisons. If the SFU value of a peptide in a sample was lower than that of the negative control peptide, it was assigned a value of zero. Such an outcome was

categorized as "unstimulated." A P value of <0.05 was considered statistically significant for all tests.

Ethics approval and consent to participate

Human PDAC resection specimens were obtained from the patients who underwent surgery at the Johns Hopkins Hospital under the Johns Hopkins Medical Institution (JHMI) Institutional Review Board (IRB) approved protocol (IRB00244430) and RAP SR at The Sidney Kimmel Comprehensive Cancer Center. This program was approved by the Johns Hopkins IRB and deemed in compliance with the Health Insurance Portability and Accountability Act.

Data availability

The dataset(s) supporting the conclusions of this article are included in the article and its additional files. Raw data is available upon request to corresponding author.

Results

Identification of variant peptides of the HLA class I–binding natural neoepitopes in the neoplastic tissues of PDAC

To understand whether natural HLA class I restricted T-cell epitopes could carry amino acid mutations, we established the *de novo* HLA class I immunopeptidome from four human PDAC tissue specimens using a previously developed mass spectrometry-based technique (31). In brief, we utilized the W6/32 monoclonal antibody affinity column to purify HLA class I complexes from PDAC tissues (32). Following the LC–MS/MS analysis of the recovered HLA class I-bound peptides, the peptide sequences were analyzed using the Novor algorithm, a *de novo* peptide sequencing algorithm. After narrowing the peptide lengths to 8 to 11 mers, we identified 2,358, 1,015, 1,040, and 1,067 unique peptides from PDAC #1, 2, 3, and 4, respectively (**Fig. 1A**). Among these, 631 (25.68%), 283 (27.88%), 311 (29.90%), and 278 (25.65%) peptides, respectively, carried a single amino acid substitution (**Fig. 1A**). By comparing these peptide sequence variants with somatic missense mutations according to WES, it was found that none of the peptide sequence variants were caused by the somatic mutations, which suggested that alternative mechanisms are involved in generating these peptide sequence variants (Supplementary Table S1).

We also examined the immunogenicity of the variant peptides. Using NetMHCPan4.0 (33), we predicted the binding affinity of the variant peptides to their respective patient's HLA-A alleles and selected 31, 3, 18, and 8 peptides, respectively, which exhibited a high binding affinity (<500 nm, a threshold routinely associated with potential immunogenicity for HLA class I restricted T cells) and at least two-fold higher affinity than their wild-type counterparts (**Fig. 1B**; Supplementary Dataset S1). We further narrowed down to 11 candidate peptides whose corresponding proteins are overexpressed in PDACs according to the Human Protein Atlas (https://www.proteinatlas.org/) and the literature (Supplementary Table S2).

Next, we performed T2-binding assays to validate the binding affinity of the synthesized peptides to their respective HLA-A alleles. This assay made use of T2 cells, which are deficient in the transporter associated with antigen processing and therefore lack the ability to transport peptide fragments into the endoplasmic reticulum to form stable peptide–HLA complexes (34). Incubation of T2 cells with exogenous peptides that binds to the HLA molecule stabilizes the molecule so that surface pMHC expression levels can be quantitatively assessed using flow cytometry. The results show that all the above-selected mutant peptides (except the PCDC4 peptide) demonstrated positive binding to the T2 cells expressing the peptide's corresponding origin HLA-A molecule (Supplementary Fig. S1A and S1B). It was found found that three variant peptides (PTPRZ1^{S1102K}, CHD9^{A2174R}, and PSMB5^{K66V}) displayed a significantly higher binding affinity compared with their wild-type counterpart (**Fig. 1C** and **D**), whereas negative peptide control was comparable to no peptide. Among these, the CHD9 variant peptide that had a binding affinity similar to the negative peptide control were excluded from the downstream analysis.

Next, we compared the immunogenicity between matched wild-type and variant peptides by performing a florospot assay to measure their ability to stimulate IFN-γ production from T cells in HLA-type-matched PBMC (HLA-A3 patient sample ID P-43 and P-20; HLA-A11 patient sample ID P-6 and P-40). PBMCs were obtained from patients from whom the variant peptides originated, which were archived before and after these patients participated in the clinical trial (NCT02451982) and received GVAX treatment (35). We anticipated that PBMC following the GVAX treatment would exhibit a higher T cell–activation signature as a result of the general stimulation of T-cell infiltration and activation by the GVAX treatment (36).

Upon stimulation with PTPRZ1^{S1102K} peptide, we detected a significantly elevated production of IFN-γ in HLA type-matched post-GVAX treatment PBMC; but this was not observed in the same PBMC stimulated with PTPRZ1 wild-type peptide (P-43: $P < 0.05$; P-20: $P < 0.05$; **Fig. 1E**). However, we did not observe any IFN-γ response following stimulation with either the PSMB5^{K66V}-mutated or PSMB5 wild-type peptide (**Fig. 1F**). Because we did not detect the PTRPZ1 epitopes in the allogenic tumor cell lines, of which the GVAX vaccine was made, it is possible that GVAX treatment induced an immune response at the tumor site, resulting in epitope spreading to the PTRPZ1 variant peptide. It is certainly also possible that the PTRPZ1 variant peptide was presented by the PDAC tumor tissues, but not presented by the tumor cell lines in the *in vitro* culture. These results suggest that variants of the HLA class I–binding natural neoepitopes are potentially immunogenic and could derive from mechanisms other than DNA mutation.

Identification of variant peptides of the HLA class I–binding natural neoepitopes in the paired neoplastic and normal tissues from the same patients with PDAC

Next, we compared the HLA class I peptides derived from tumor tissues to those from matched normal tissues from the same patients to understand the cancer specificity of the above-identified wild-type and variant peptides. We extracted and compared the immunopeptidome of 16 paired PDAC-normal tissue specimens from 15 patients (Supplementary Table S3). These 16 paired fully deidentified specimens were archived either through the RAP SR at the Sidney Kimmel Comprehensive Cancer Center at Johns Hopkins (SKCCC) or from patients who underwent surgery at the Johns Hopkins Hospital. Among them, nine were primary tumors and paired with normal pancreas; seven pairs were tumors from metastases (two from the lung, five from the liver) and their respective normal tissues.

Using the MaxQuant algorithm, which matches the MS/MS spectrum of the purified peptides to the existing reference normal protein library (UniProtKB Proteome UP000005640), a total of 8,094 unique HLA class I–binding peptides were identified from the tumor tissues and 11,250 unique peptides from normal tissues. The length histogram shows a wide distribution of peptide length, but

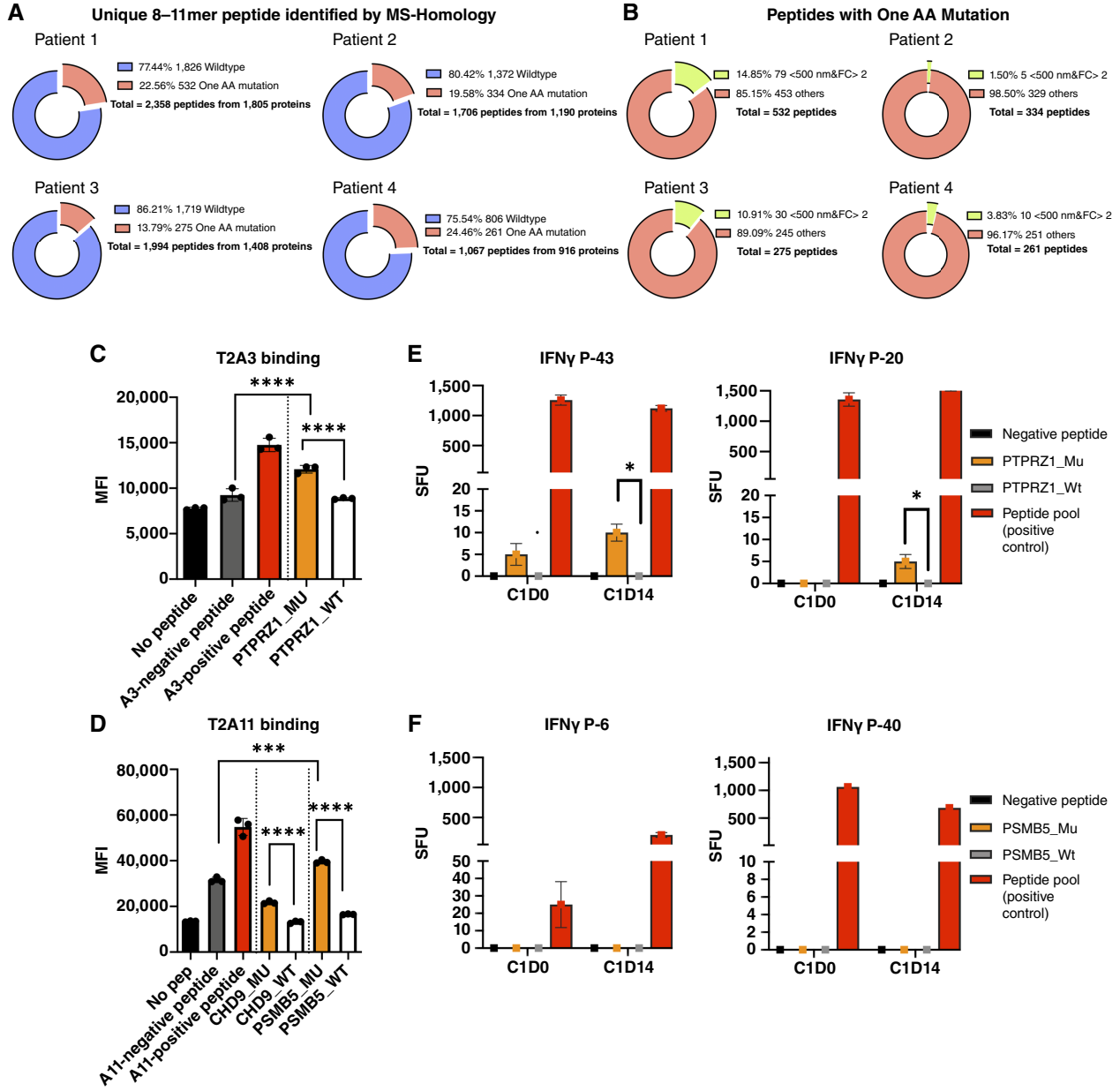

Figure 1.

Identification of immunogenic HLA class I–bound variant peptides with single amino acid substitution from patient PDAC tumor specimen. Novor *de novo* sequencing software was used to sequence the tandem MS data of HLA class I peptide from the patient's PDAC tumor. MS-Homology was used to identify peptides carrying a single amino acid substitution. NetMHCpan4.0 was used to predict peptide binding affinity to their respective HLA molecule. (**A**) Variant peptides identified in four patient PDAC samples and (**B**) selected strong binding variant peptides. (**C**) T2 cell binding assays of selected HLA-A3 and (**D**) A11 peptides binding to HLA-A3 or HLA-A11 expressing T2 cells. T2 cells expressing HLA-A3 or HLA-A11 molecules were incubated with B2 M (1.5 μg/mL) and their respective peptides (50 μg/mL) in an equal mix of serum-free AimV medium and RPMI1640-based culture media at room temperature with gentle shaking overnight. Negative peptide and positive peptide control for HLA-A3 and HLA-A11 is CEF1(GILGFVFTL) and CEF3(SIIPSGPLK), respectively. An unpaired *t* test was used for comparing the MFI of different peptides. (**E**) and (**F**) Florospot assay measuring the number of T cells producing IFNγ in GVAX-treated (HLA-A3 patient sample ID P-43 and P-20; HLA-A11 patient sample ID P-6 and P-40) PBMC following stimulation with PTPRZ1 or PSMB5 peptides, respectively. C1D0 samples are pre-GVAX-treated PBMC, and C1D14 samples are PBMC collected 14 days post-GVAX treatment. SFU is the number of spots per 10^6 PBMCs. Unpaired *t* test and one-way analysis of variance were used for comparing stimulated and unstimulated peptide/samples. *, $P < 0.05$; ***, $P < 0.001$; ****, $P < 0.0001$.

the peak length for almost all specimens is nine amino acids, which is the expected length of HLA class I epitopes (**Fig. 2A**; Supplementary Fig. S2; Supplementary Table S4; ref. 37). Using the Novor *de novo* sequencing software, a total of 250,751 unique peptides from the tumor tissues and 241,212 peptides from normal tissues were identified. The length histogram again peaked at nine amino

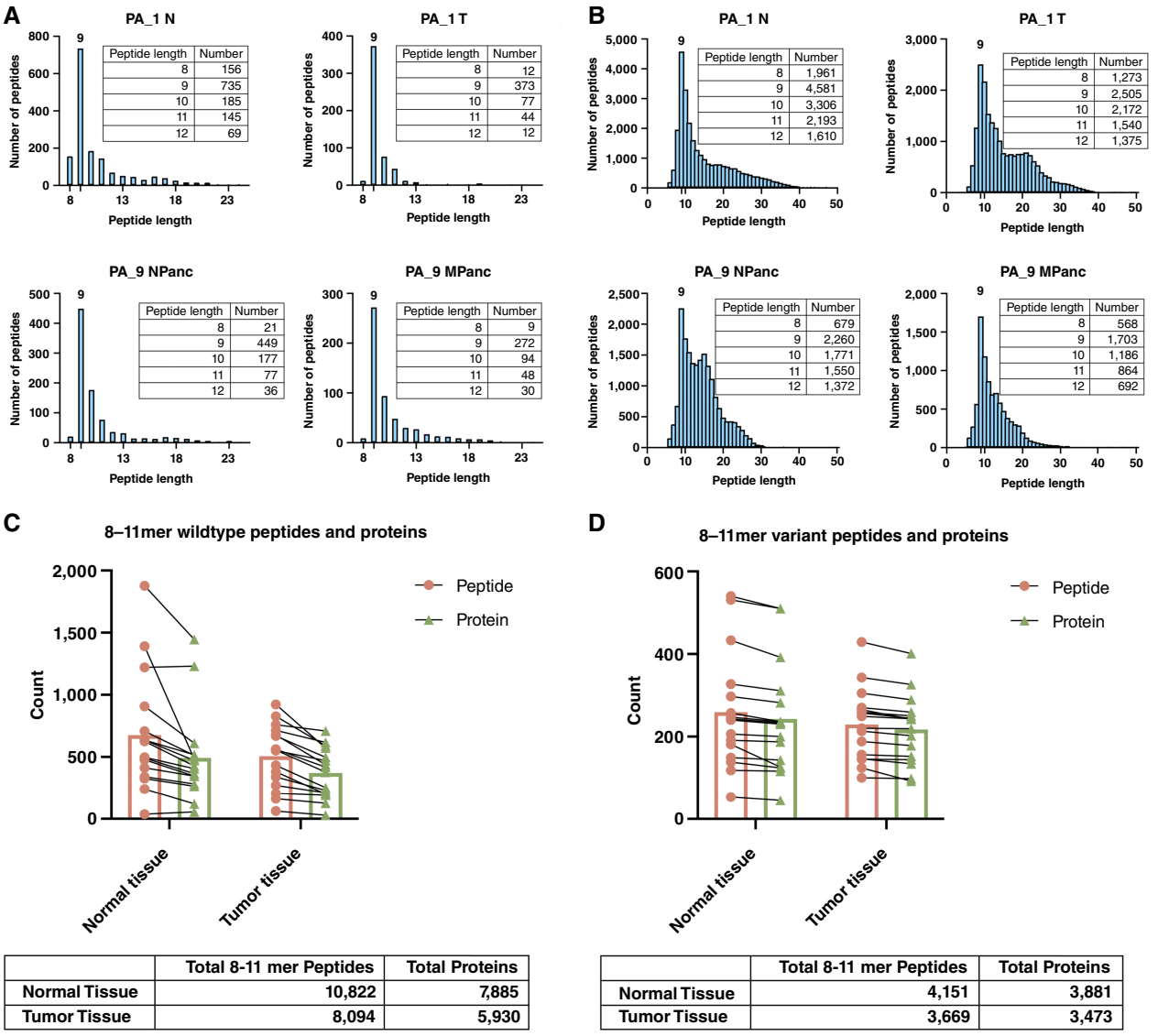

	Total 8-11 mer Peptides	Total Proteins
Normal Tissue	10,822	7,885
Tumor Tissue	8,094	5,930

	Total 8-11 mer Peptides	Total Proteins
Normal Tissue	4,151	3,881
Tumor Tissue	3,669	3,473

Figure 2.

Identification of HLA class I–bound peptides from patient PDAC tumor specimen and matched normal tissue specimen. Histograms show representative length distribution of (**A**) MaxQuant database searched peptides and (**B**) Novor *de novo* sequencing searched peptides from PA_1 and PA_9. The numbers of peptides and proteins identified in both tumor and paired normal specimens ($n = 16$) using (**C**) MaxQuant database search and (**D**) Novor *de novo* sequencing search are shown. Each line matching a set of peptide and protein counts symbolizes one patient. The total number of 8–11 mer peptides and total protein content were calculated by summing the individual amounts of each peptide and protein from all 16 normal or tumor specimens. Proteins from which the peptides are derived were identified using MS-Homology (http://prospector.ucsf.edu).

acids for essentially all the specimens (**Fig. 2B**; Supplementary Fig. S3).

Because the canonical HLA class I epitope is 8 to 11 amino acids long (37–39), our peptidome pool was narrowed to include only peptides within this length range. Within the MaxQuant-identified peptide pool, we identified a total of 10,822 unique 8 to 11 mer peptides from 7,885 unique source proteins in the normal tissues and a total of 8,094 unique 8 to 11 mer peptides from 5,930 unique source proteins in the tumor tissues (**Fig. 2C**). We then filtered the Novor *de novo* identified peptides within this length range for a single amino acid substitute. From the pool of peptides analyzed *de novo*, we identified 4,151 unique 8 to 11 mer variant peptides from 3,881 unique source proteins in normal tissues and 3,669 unique 8 to 11 mer variant peptides from 3,473 unique source proteins in tumor tissues (**Fig. 2D**).

Tumor-specific variant peptides are shared among multiple patients

Next, we compared the immunopeptidome of each pair of tumor and normal tissues to identify tumor-specific 8 to 11 mer peptides. Across all 16 pairs of specimens, we found that an average of 65.3% (SD = 15.6%) of wild-type peptides and 92.5% (SD = 4.2%) of variant peptides extracted from the tumor tissues were unique to tumor tissues (**Fig. 3A**; Supplementary Tables S4 and S5) even

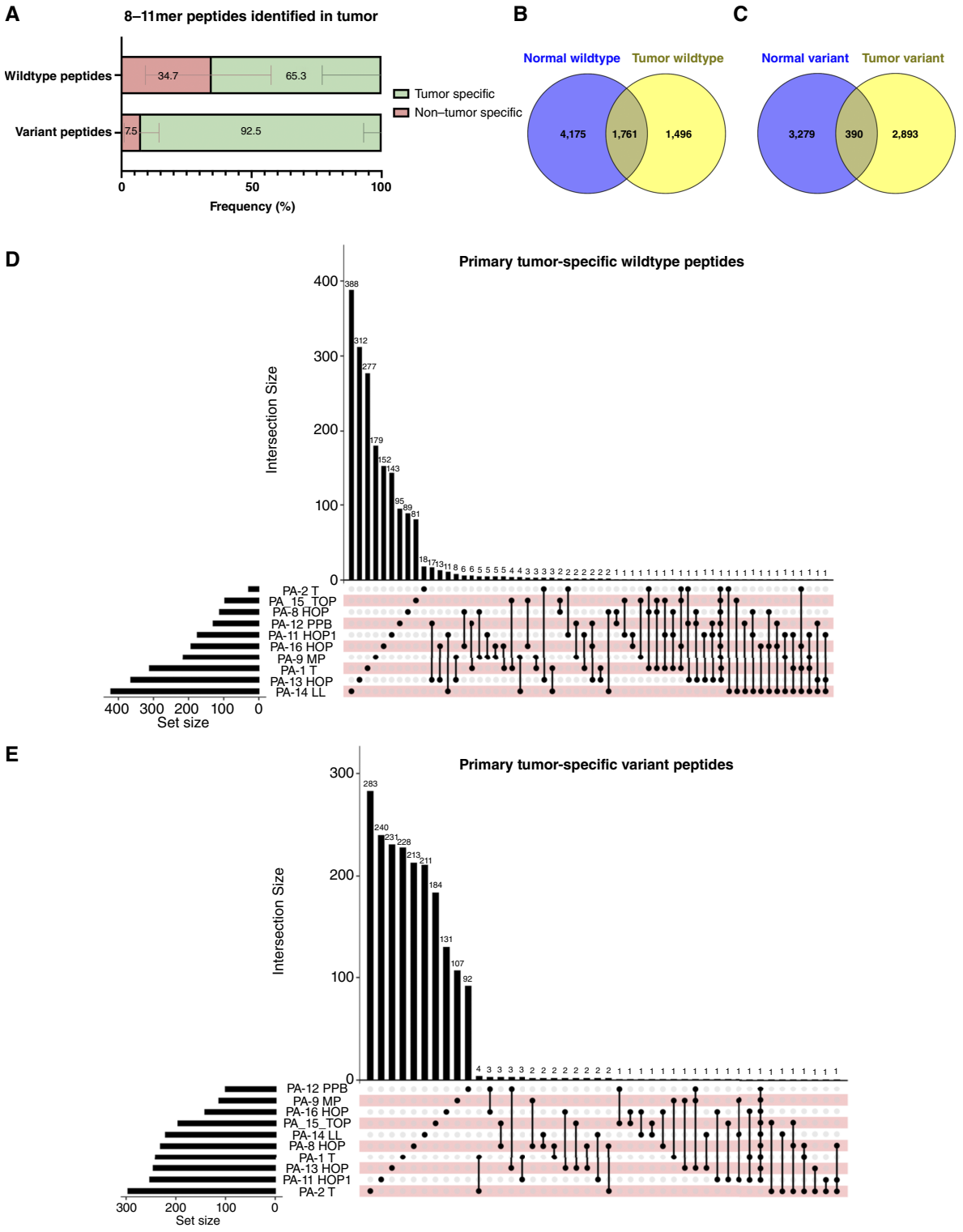

Figure 3.

PDAC-specific HLA class I–bound wild-type and variant peptides. (**A**) Percentage of tumor-specific and non–tumor specific wild-type and variant peptides extracted from tumor tissues. A peptide is considered tumor specific if it is not found within the peptide pool of the normal tissue specimens. Non–tumor-specific peptides are those peptides that are found in both tumor and normal tissue-specimen peptide pools. Data are shown as mean ± SD. Venn diagram showing overlap between tumor and normal tissue's unique wild-type (**B**) and variant peptides (**C**). UpSet plot showing (**D**) wild-type and (**E**) variant peptides shared between primary tumor specimens.

though slightly fewer unique variant peptides were found in the tumor tissues. This finding also suggests that variant peptides are particularly tumor specific in the majority of patients although the same variant peptides can be found in the normal tissues of a few patients. Interestingly, among all unique wild-type 8 to 11 mer peptides, 4,175 were found in normal tissues, 1,496 in tumor tissues, and 1,761 were shared between normal and tumor tissues (**Fig. 3B**). In contrast, among variant 8 to 11 mer peptides, 3,279 were found in normal tissues, 2,893 in tumor tissues, with only 390 shared between normal and tumor tissues (**Fig. 3C**). These analyses, combined with those in **Fig. 3A**, suggest that a subgroup of unique wild-type and variant peptides is more enriched in tumor tissues. The increased percentage of tumor-specific, wild-type, and variant peptides shown in **Fig. 3A** is due to the repeated occurrence of such a subgroup of peptides in tumors.

We subsequently compared the tumor-specific immunopeptidome among tumor tissues from either primary PDAC or from metastatic sites to identify tumor-shared antigens in PDACs. We found that, among primary PDAC specimens, 19 wild-type peptides (1.01% of total tumor-specific wild-type peptides) were shared by three or more PDACs, and 122 wild-type peptides (6.51%) were shared between two PDACs (**Fig. 3D**). In addition, six variant peptides (0.3% of total tumor-specific variant peptides) were shared between three or more PDACs, and 46 variant peptides (2.33%) were shared between two PDACs (**Fig. 3E**). Interestingly, one variant peptide (ETALVELVK; Albumin^{E550Q}) was found to be shared among nine patients. However, because of the nature of the protein's ubiquitous expression, we believe it has limited therapeutic target value, and thus did not investigate further. Among metastatic PDAC specimens, 55 wild-type peptides (2.56% of tutor tumor specific wild-type peptides) were shared by three or more PDACs, and 292 wild-type peptides (13.61%) were shared between two PDACs (Supplementary Fig. S4A). For variant peptides, three peptides (0.26% of total tumor-specific variant peptides) were shared between three or more PDACs, and 36 peptides (2.72%) were shared between two PDACs (Supplementary Fig. S4B). We were also interested in seeing whether shared tumor antigens existed in tumor tissues from both primary and metastatic sites in the same patient. By comparing the peptides extracted from both the primary and metastatic tumor (lung) in patient 15, we found 21 wild-type (Supplementary Fig. S5A), and four variant peptides (Supplementary Fig. S5B) were shared by both specimens. Taken together, these results suggest that variant peptides are largely tumor specific within individual patients and shared among multiple patients.

Patterns of the amino acid substitutions in the HLA class I–binding variant peptides

We examined the top 10 most frequent AA substitutions of the variant peptides specific to either normal tissue or tumor tissues. We observed a similar AA substitution pattern in both tumor-specific variant peptides and normal tissue-specific variant peptides, with Q-E (20.44% in normal tissue-specific variant peptides; 24.59% in tumor-specific variant peptides), N-D (23.56% in normal tissue-specific variant peptides; 19.89% in tumor-specific variant peptides), and V-L (11.33% in normal tissue-specific variant peptides; 16.85% in tumor-specific variant peptides), making up the top three most frequent substitutions in both tumor and normal tissue-specific variants peptides (**Fig. 4A** and **B**).

Although the most frequent AA substitutions are the same between tumor and normal tissue-specific variant peptides, we found that quite a few types of AA substitutions were only observed among the top 10 types of substitutions in tumor-specific variant peptides (**Fig. 4B**). Next, we investigate whether tumor-specific AA substitutions would influence the immunogenicity of variant peptides. We identified 41 normal tissue-specific variant (0.96%; **Fig. 4C**; Supplementary Table S6) and 45 tumor-specific variant

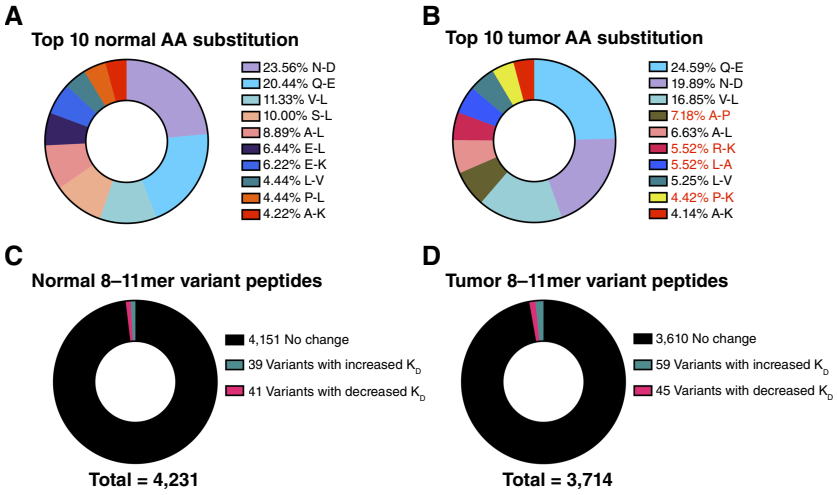

Figure 4.

Properties of normal and tumor-specific variant peptides. (**A**) and (**B**) show the top 10 AA substitution patterns in the variant peptide pool of normal and tumor specimens, respectively. The percentage shown is out of the total peptides that contain one of these top 10 AA substitutions. AA substitutions only found within tumor samples' top 10 substitutions are highlighted in red. AA substitutions were identified using MS-Homology (http://prospector.ucsf.edu). (**C**) and (**D**) show the number of variant peptides with increased and decreased binding affinity (K_D) identified in normal and tumor tissues, respectively. Variant peptides with decreased K_D are defined as those with (1) K_D below 500 nmol/L and (2) at least two-fold lower K_D compared with its wild-type counterpart. Variant peptides with increased K_D are defined as those with (1) wild-type counterpart peptide with K_D below 500 nmol/L and (2) at least two-fold higher K_D compared with its wild-type counterpart. BA was predicted using NetMHCpan4.0.

peptides (1.21%; **Fig. 4D**; Supplementary Table S7) with a strong predicted HLA class I–binding affinity (<500 nm) and an at least two-fold increased binding affinity compared with their wild-type counterparts. Although very few variant peptides from tumor tissues had an increased binding affinity compared with their wild-type counterparts, these peptides are potentially more immunogenic and should be further investigated as immunotherapy targets. Interestingly, some AA substitutions significantly decreased the binding affinity of the peptides. We identified 39 normal tissue-specific variant peptides (0.92%; **Fig. 4C**; Supplementary Table S8) and 59 tumor-specific variant peptides (1.59%; **Fig. 4D**; Supplementary Table S9) whose wild-type counterpart peptides scored a strong HLA class I–binding affinity (<500 nm) and an at least two-fold decreased binding affinity compared with their wild-type counterparts. The low binding affinity of the majority of the variant peptides in both tumor and normal tissues could potentially lead to an immune evasion.

Structure basis of altered binding affinity between variant peptide and HLA

To understand how a variant peptide can increase binding affinity to HLA, we performed molecular modeling of a normal and neoepitope actin peptide in complex with the respective HLA class I molecule, HLA-A*33:01. AlphaFold (29, 40) in the Google's CoLab was used to predict the structure with high confidence (Supplementary Figs. S6A and S6B, S7A and S7B). The wild-type actin peptide had a predicted binding affinity of 2.8 μmol/L, whereas its variant counterpart had a much higher predicted binding affinity of 0.5 μmol/L. The single substitution at Position 1 of the peptide (G to Q) did not alter the three-dimensional peptide-MHC structure, with the RMSD between two peptides at 0.14 Å (Supplementary Fig. S8). However, in the variant peptide, the sidechain amide nitrogen of Q1 forms a hydrogen with carbonyl of G2 carbonyl. This new hydrogen bond, as absent in the normal peptide, can likely account for the increase in binding affinity for the variant peptide. Similar structural mechanisms may account for altered affinities presented in this paper.

Discussion

To the best of our knowledge, this is the first study that compared the immunopeptidome of PDAC tissues and matched normal tissues from the same patients. We were able to identify natural HLA class I–binding variant peptides with single amino acid substitutes not because of genetic variants. The findings also suggest that noncanonical neoantigens may arise from translational errors. Because these variant peptides are largely tumor specific within individual patients and shared among multiple patients, and because some of them are potentially more immunogenic than their wild-type counterparts, they may be neoantigen candidates for vaccine and T-cell therapy development. As a future direction, it is vital to investigate how T-cell recognition translates into specific reactivity against tumor cells presenting natural levels of MHC I/peptide complexes. Although this aspect was not addressed in the present study, we have been actively developing mRNA vaccines that express these epitopes, aiming to generate *in vivo* data that will deepen our understanding of T-cell responses in the tumor microenvironment.

Although only a limited number of PDAC tissues had matched tumor WES data, this study suggests that identified HLA class I–binding variant peptides do not arise from genomic mutations. This notion is further supported by the presence of variant peptides in normal tissues.

We hypothesize that the variant peptides observed in our study could be derived from a specific type of DRiPs, namely those resulting from tRNA-amino acid misacylation errors during protein synthesis. Although DRiPs typically result from additions or deletions of amino acids due to various mechanisms, tRNA-amino acid misacylation can cause specific single amino-acid substitutions in peptides (41). Although proteasome splicing could potentially contribute to the observed substitutions, it is less likely to account for the diversity of substitutions we have observed. Therefore, we propose that the single amino-acid substitutions in our study are most likely caused by translation errors involving tRNA-amino acid misacylation. Mutations in the tRNA binding pocket of aminoacyl-tRNA synthetases, mutations in amino-acid-binding pocket of aminoacyl-tRNA synthetases, and amino acid imbalance are anticipated to cause the substitutions of any amino acid. A mischarged target recognized by aminoacyl-tRNA synthetases or by trans-editing factors would lead to a specific type of amino acid substitution. It is likely that the observed diversity of amino acid substitutions is attributable to multiple translation editing mechanisms. Whether these potential mechanisms account for the observed variant peptide remains to be substantiated.

Although variant peptides, if caused by translation errors, are anticipated to be observed in normal tissues, this study suggests that most variant peptides occur more frequently in tumor tissues. These results suggest that cancer-specific mechanisms may account for those cancer-specific variant peptides and are worth exploring. Furthermore, the noncanonical neoepitopes observed in this study were found to be shared among multiple patients. Therefore, the neoepitopes observed in this study are promising neoantigen candidates for vaccine and T-cell therapy development.

Authors' Disclosures

M. Hill reports non-financial support from Bristol-Myers Squibb outside the submitted work; in addition, M. Hill is an employee of Bristol-Myers Squibb, which funded the research. L. Zheng reports grants from Bristol-Myers Squibb, Merck, AstraZeneca, iTeos, Amgen, NovaRock, Inxmed, Halozyme and Abmeta and personal fees from Biosion, Alphamab, NovaRock, Ambrx, Akrevia/Xilio, QED, Novagenesis, Snow Lake Capitals, Amberstone, Pfizer, Tavotek, Mingruizhiyao, and Cellaration outside the submitted work. No disclosures were reported by the other authors.

Authors' Contributions

T. Zhang: Data curation, formal analysis, validation, investigation, visualization, methodology, writing–original draft, writing–review and editing. **B. Celiker:** Data curation, formal analysis. **Y. Shao:** Data curation. **J. Gai:** Data curation. **M. Hill:** Supervision. **C. Wang:** Supervision, writing–review and editing. **L. Zheng:** Conceptualization, resources, supervision, funding acquisition, methodology, project administration, writing–review and editing.

Acknowledgments

We would like to acknowledge the important insight provided by Irene Jarchum, Auditi DebRoy, and Cameron Brandt from the Bristol-Myers Squibb group. This work was done at the Johns Hopkins University. This study was supported by a Bristol-Myers Squibb II-ON grant (L. Zheng). L. Zheng is supported by NIH Grant R01 CA169702, NIH Grant R01 CA197296, NIH Grant P01 CA247886, NIH SPORE Grant P50 CA062924, and NIH Cancer Center Support Grant P30 CA006973.

Note

Supplementary data for this article are available at Clinical Cancer Research Online (http://clincancerres.aacrjournals.org/).

Received July 14, 2024; revised October 4, 2024; accepted December 17, 2024; posted first December 19, 2024.

References

1. Rahib L, Wehner MR, Matrisian LM, Nead KT. Estimated projection of US cancer incidence and death to 2040. JAMA Netw Open 2021;4:e214708.
2. Halbrook CJ, Lyssiotis CA, Pasca di Magliano M, Maitra A. Pancreatic cancer: advances and challenges. Cell 2023;186:1729–54.
3. Timmer FEF, Geboers B, Nieuwenhuizen S, Dijkstra M, Schouten EAC, Puijk RS, et al. Pancreatic cancer and immunotherapy: a clinical overview. Cancers (Basel) 2021;13:4138.
4. Ho WJ, Jaffee EM, Zheng L. The tumour microenvironment in pancreatic cancer—clinical challenges and opportunities. Nat Rev Clin Oncol 2020;17:527–40.
5. Marofi F, Motavalli R, Safonov VA, Thangavelu L, Yumashev AV, Alexander M, et al. CAR T cells in solid tumors: challenges and opportunities. Stem Cell Res Ther 2021;12:81.
6. Newick K, O'Brien S, Moon E, Albelda SM. CAR T cell therapy for solid tumors. Annu Rev Med 2017;68:139–52.
7. Thind K, Padrnos LJ, Ramanathan RK, Borad MJ. Immunotherapy in pancreatic cancer treatment: a new frontier. Therap Adv Gastroenterol 2017;10:168–94.
8. Leko V, Rosenberg SA. Identifying and targeting human tumor antigens for T cell-based immunotherapy of solid tumors. Cancer Cell 2020;38:454–72.
9. Xie N, Shen G, Gao W, Huang Z, Huang C, Fu L. Neoantigens: promising targets for cancer therapy. Signal Transduct Target Ther 2023;8:9.
10. Chan AY, Anderson MS. Central tolerance to self revealed by the autoimmune regulator. Ann N Y Acad Sci 2015;1356:80–9.
11. Smith CC, Selitsky SR, Chai S, Armistead PM, Vincent BG, Serody JS. Alternative tumour-specific antigens. Nat Rev Cancer 2019;19:465–78.
12. Rojas LA, Sethna Z, Soares KC, Olcese C, Pang N, Patterson E, et al. Personalized RNA neoantigen vaccines stimulate T cells in pancreatic cancer. Nature 2023;618:144–50.
13. Chen H, Yang G, Xiao J, Zheng L, You L, Zhang T. Neoantigen-based immunotherapy in pancreatic ductal adenocarcinoma (PDAC). Cancer Lett 2020;490:12–9.
14. Fotakis G, Trajanoski Z, Rieder D. Computational cancer neoantigen prediction: current status and recent advances. Immunooncol Technol 2021;12:100052.
15. Feola S, Chiaro J, Martins B, Cerullo V. Uncovering the tumor antigen landscape: what to know about the discovery process. Cancers (Basel) 2020;12:1660.
16. Liepe J, Marino F, Sidney J, Jeko A, Bunting DE, Sette A, et al. A large fraction of HLA class I ligands are proteasome-generated spliced peptides. Science 2016;354:354–8.
17. Rock KL, Farfán-Arribas DJ, Colbert JD, Goldberg AL. Re-examining class-I presentation and the DRiP hypothesis. Trends Immunol 2014;35:144–52.
18. Engelhard VH, Altrich-Vanlith M, Ostankovitch M, Zarling AL. Post-translational modifications of naturally processed MHC-binding epitopes. Curr Opin Immunol 2006;18:92–7.
19. Hoyos LE, Abdel-Wahab O. Cancer-specific splicing changes and the potential for splicing-derived neoantigens. Cancer Cell 2018;34:181–3.
20. Mordret E, Dahan O, Asraf O, Rak R, Yehonadav A, Barnabas GD, et al. Systematic detection of amino acid substitutions in proteomes reveals mechanistic basis of ribosome errors and selection for translation fidelity. Mol Cell 2019;75:427–41.e5.
21. Pataskar A, Champagne J, Nagel R, Kenski J, Laos M, Michaux J, et al. Tryptophan depletion results in tryptophan-to-phenylalanine substitutants. Nature 2022;603:721–7.
22. Wang J, Zhang T, Li P, Gai J, Chen S, Espinoza G, et al. Engineered TCR T-cell therapy targeting mass spectrometry-identified natural epitope in PDAC. Cancer Lett 2023;573:216366.
23. Ma B. Novor: real-time peptide de novo sequencing software. J Am Soc Mass Spectrom 2015;26:1885–94.
24. Bassani-Sternberg M. Mass spectrometry based immunopeptidomics for the discovery of cancer neoantigens. Methods Mol Biol 2018;1719:209–21.
25. Rozanov DV, Rozanov ND, Chiotti KE, Reddy A, Wilmarth PA, David LL, et al. MHC class I loaded ligands from breast cancer cell lines: a potential HLA-I-typed antigen collection. J Proteomics 2018;176:13–23.
26. Bassani-Sternberg M, Bräunlein E, Klar R, Engleitner T, Sinitcyn P, Audehm S, et al. Direct identification of clinically relevant neoepitopes presented on native human melanoma tissue by mass spectrometry. Nat Commun 2016;7:13404.
27. Zhang M, Pan X, Fujiwara K, Jurcak N, Muth S, Zhou J, et al. Pancreatic cancer cells render tumor-associated macrophages metabolically reprogrammed by a GARP and DNA methylation-mediated mechanism. Signal Transduct Target Ther 2021;6:366.
28. Cox J, Mann M. MaxQuant enables high peptide identification rates, individualized p.p.b.-range mass accuracies and proteome-wide protein quantification. Nat Biotechnol 2008;26:1367–72.
29. Ruff KM, Pappu RV. AlphaFold and implications for intrinsically disordered proteins. J Mol Biol 2021;433:167208.
30. Mirdita M, Schütze K, Moriwaki Y, Heo L, Ovchinnikov S, Steinegger M. ColabFold: making protein folding accessible to all. Nat Methods 2022;19:679–82.
31. Fujiwara K, Shao Y, Niu N, Zhang T, Herbst B, Henderson M, et al. Direct identification of HLA class I and class II-restricted T cell epitopes in pancreatic cancer tissues by mass spectrometry. J Hematol Oncol 2022;15:154.
32. Barnstable CJ, Bodmer WF, Brown G, Galfre G, Milstein C, Williams AF, et al. Production of monoclonal antibodies to group A erythrocytes, HLA and other human cell surface antigens-new tools for genetic analysis. Cell 1978;14:9–20.
33. Jurtz V, Paul S, Andreatta M, Marcatili P, Peters B, Nielsen M. NetMHCpan-4.0: improved peptide-MHC class I interaction predictions integrating eluted ligand and peptide binding affinity data. J Immunol 2017;199:3360–8.
34. Henderson RA, Michel H, Sakaguchi K, Shabanowitz J, Appella E, Hunt DF, et al. HLA-A2.1-associated peptides from a mutant cell line: a second pathway of antigen presentation. Science 1992;255:1264–6.
35. Heumann T, Judkins C, Li K, Lim SJ, Hoare J, Parkinson R, et al. A platform trial of neoadjuvant and adjuvant antitumor vaccination alone or in combination with PD-1 antagonist and CD137 agonist antibodies in patients with resectable pancreatic adenocarcinoma. Nat Commun 2023;14:3650.
36. Lutz ER, Wu AA, Bigelow E, Sharma R, Mo G, Soares K, et al. Immunotherapy converts nonimmunogenic pancreatic tumors into immunogenic foci of immune regulation. Cancer Immunol Res 2014;2:616–31.
37. Gfeller D, Guillaume P, Michaux J, Pak H-S, Daniel RT, Racle J, et al. The length distribution and multiple specificity of naturally presented HLA-I ligands. J Immunol 2018;201:3705–16.
38. Granados DP, Sriranganadane D, Daouda T, Zieger A, Laumont CM, Caron-Lizotte O, et al. Impact of genomic polymorphisms on the repertoire of human MHC class I-associated peptides. Nat Commun 2014;5:3600.
39. Trolle T, McMurtrey CP, Sidney J, Bardet W, Osborn SC, Kaever T, et al. The length distribution of class I-restricted T cell epitopes is determined by both peptide supply and MHC allele-specific binding preference. J Immunol 2016;196:1480–7.
40. Jumper J, Evans R, Pritzel A, Green T, Figurnov M, Ronneberger O, et al. Highly accurate protein structure prediction with AlphaFold. Nature 2021;596:583–9.
41. Antón LC, Yewdell JW. Translating DRiPs: MHC class I immunosurveillance of pathogens and tumors. J Leukoc Biol 2014;95:551–62.